

Elsevier Editorial System(tm) for Deep-Sea Research Part II
Manuscript Draft

Manuscript Number:

Title: Circulation, stratification and seamounts in the South West Indian Ocean

Article Type: SW Indian Ocean Ridge

Keywords: ocean circulation
subtropical gyre
mesoscale eddies
seamounts
Agulhas Current
Southwest Indian Ocean (20-45°S, 25-60°E)

Corresponding Author: Prof. Raymond Trevor Pollard, PhD

Corresponding Author's Institution: National Oceanography Centre

First Author: Raymond Trevor Pollard, PhD

Order of Authors: Raymond Trevor Pollard, PhD; Jane F Read

1

2

3

4 **Circulation, stratification and seamounts in the South**
5 **West Indian Ocean**

6

7

8

9

10 Raymond Pollard¹ and Jane Read¹

11

12

13

14

15

16

17

18

19

20

21

22 ¹National Oceanography Centre

23 University of Southampton Waterfront Campus

24 European Way

25 Southampton SO14 3ZH

26 United Kingdom

27

28 Corresponding author: raymond.pollard@gmail.com

29 telephone: +44 1590682118

30

Abstract

31 Circulation in the vicinity of six seamounts along the Southwest Indian Ridge was studied
32 as part of a multidisciplinary survey in November 2009. Examination of altimetric data
33 shows that several of the seamounts lie in the area of slow mean westward flow between
34 the southern tip of Madagascar (25°S) and the Agulhas Return Current (ARC) flowing
35 eastward between 37-40°S. The mean westward drift of mesoscale features was 4.1 ± 0.9
36 cm s^{-1} . Integrated between Madagascar and 37°S, this westward drift can account for 50
37 Sv ($1 \text{ Sv} = 10^6 \text{ m}^3 \text{ s}^{-1}$), which, added to 25 Sv of southward flow past Madagascar, is
38 sufficient to account for the total Agulhas Current transport of 70 ± 21 Sv. The transport
39 of the ARC was also measured, at two longitudes, down to 2000 m. Combined with
40 earlier crossings of the ARC in 1986 and 1995, the full depth transport of the ARC is
41 estimated at 71 – 85 Sv at longitudes 40 – 50°E, indicating that the Agulhas Current then
42 ARC transport continues unreduced as far as 50°E before beginning to recirculate in the
43 Southwest Indian Ocean subtropical gyre. The primary control on the circulation near
44 each seamount was its position relative to any mesoscale eddy at the time of the survey.
45 Melville lay on the flank of a cyclonic eddy that had broken off the ARC and was
46 propagating west before remerging with the next meander of the ARC. Nearby Sapmer,
47 on the other hand, was in the centre of an anticyclonic eddy, resulting in very weak
48 stratification over the seamount at the time of the survey. Middle of What lies most often
49 on the northern flank of the ARC, in strong currents, but was at the time of the survey
50 near the edge of the same eddy as Sapmer. Coral, in the Subtropical Front south of the
51 ARC, was in waters much colder, fresher, denser and more oxygenated than all the other
52 seamounts. Walter was close to the path of eddies propagating southwest from east of
53 Madagascar, while Atlantis, the furthest east and north seamount, experienced the
54 weakest eddy currents.

55 Keywords

56 Ocean circulation subtropical gyre; mesoscale eddies; seamounts;
57 Agulhas Return Current; Southwest Indian Ocean (20 – 45°S, 25 – 60°E)

58

1. Introduction

59 In late 2009, the research vessel *Dr. Fridtjof Nansen* carried out a 6-week multi-
60 disciplinary survey of six seamounts in the Southwest Indian Ocean (**Fig. 1**). The purpose
61 of this paper is to summarize the mean circulation and the role of mesoscale eddies in
62 modifying the circulation and stratification at each seamount at the time of the cruise.

63 Six seamounts were surveyed (**Table 1**), five of which lay along the line of the Southwest
64 Indian Ridge (Fig. 1), which is split by deep fracture zones. Atlantis, Melville and Coral
65 seamounts were situated on ridges just east of the Atlantis, Indomed and Discovery II
66 Fracture Zones respectively; Sapmer was just west of the Gallieni Fracture Zone; Middle
67 of What (MoW) was a deeper feature on the ridge between Melville and Sapmer. Walter
68 was another deep feature situated on the west side of the Madagascar Ridge, and
69 northwest of the Walter's Shoals, the shallowest part of the Ridge.

70 A limited number of physical oceanographic observations were made at each seamount,
71 including a short CTD section and a 24-hour CTD yoyo. A few CTD stations were also
72 occupied on passage and two CTD sections across the Agulhas Return Current (ARC)

73 were worked. Shipboard acoustic Doppler current profiler (ADCP) data were acquired
74 throughout the cruise. Shipboard data have been supplemented with Maps of Absolute
75 Dynamic Topography (MADT) (**Fig. 2**), obtained from the SSALTO/DUACS (Segment
76 Sol multimissions d'ALTimétrie, d'Orbitographie et de localisation précise/Developing
77 Use of Altimetry for Climate Studies) multimission altimeter data processing system,
78 distributed by CLS/AVISO (Collecte Localis Satellites/Archivage, Validation,
79 Interprétation des données des Satellite Océanographiques). Fig. 2a shows the synoptic
80 surface circulation on 18 November 2009, when the first seamount, Atlantis, was being
81 surveyed. Four weeks later (Fig. 2b), the survey of the final seamount, Walter, had just
82 ended.

83 The best known current in the Southwest Indian Ocean is the Agulhas Current
84 (Lutjeharms, 2006), running to the southwest down the east coast of South Africa (Fig.
85 2). To the south of Africa, the Agulhas Current retroflects to the east, meandering
86 between 37°S and 41°S in the Agulhas Return Current (ARC). The ARC weakens to the
87 east as transport peels off to the north (Lutjeharms, 2007; Stramma and Lutjeharms,
88 1997) to close the anticyclonic (anticlockwise) Southwest Indian Ocean Subtropical Gyre.
89 South of the ARC, two areas of closely spaced sea surface height (SSH) contours can be
90 identified (Fig. 2), marking the Subtropical Front (STF) (Belkin and Gordon, 1996; Read
91 *et al.*, 2000) and the Subantarctic Front (SAF). The SAF is marked by the tightening of
92 SSH contours just east of Coral (Fig. 2, transition from green to yellow), and is the
93 northern edge of the Antarctic Circumpolar Current (ACC), which reaches its
94 northernmost circumpolar excursion at 50°E (Pollard and Read, 2001; Pollard *et al.*,
95 2007). Thus Coral seamount lies just north of the ACC but in the path of the STF and, on
96 occasion, the ARC (Boebel *et al.*, 2003).

97 **2. Eastward transport along the southern boundary of the Subtropical Gyre**

98 Two closely spaced hydrographic sections (Fig. 2), between Coral and Melville (33 km
99 station spacing) and south of MoW (28 km spacing), allow us to identify the ARC, STF
100 and SAF and estimate their boundaries and separate eastward transports. Using
101 temperature and salinity range criteria for these fronts at several depths (Belkin and
102 Gordon, 1996) and the 300 – 800 m depth range for the 10°C isotherm to identify the
103 ARC (Belkin and Gordon, 1996), we have identified the CTDs nearest to the boundaries
104 between the ARC, STF and SAF and overlaid them on the sea surface height contours of
105 Fig. 2b (**Fig. 3**). The bold dashed lines in Fig. 3 connect these CTDs following sea
106 surface height contours. There are only small offsets between the estimated frontal
107 boundaries and the sea surface height contours on each section, so our choice of frontal
108 boundaries is consistent between the two sections.

109 Geostrophic transports for adjacent station pairs (Fig. 3) have been calculated down to
110 1500 m relative to 1500 m for comparison with other estimates (Lutjeharms and Anson, 2001).
111 Note the transport minimum between the ARC and STF on each section (2.9 and
112 3.0 Sv on west and east sections respectively), which indicates a separation between the
113 ARC and STF transports. However, there is no minimum between STF and the SAF (seen
114 only on the eastern section) so we cannot reliably apportion the transport between the
115 two.

116 Transports for the ARC are 44 and 51 Sv for the 45°E and 50°E sections (Fig. 3). The
117 difference between these estimates could have several explanations. The anticyclonic
118 eddy around Sapmer and the large gap between MoW and the next station to the south
119 could have increased the transport for the eastern section. Transports could have changed
120 during the week that elapsed between the occupations of the two sections. For
121 comparison, the transport of the Agulhas Current was observed to change from its
122 minimum 9 Sv to its maximum 122 Sv in only 24 days (Bryden *et al.*, 2005) so changes
123 of over 4 Sv per day are observed. Our ARC transports are consistent with previous
124 estimates. For *RRS Discovery* cruise 164 (Read and Pollard, 1993) in 1986 the equivalent
125 (above 1500 m) ARC transport across 40°E was 49 Sv (calculated as 42 Sv by
126 (Lutjeharms and Ansorge, 2001). For *Discovery* cruise 213 (Pollard and Read, 2001) in
127 1995 the ARC transport across 41°E was 44 Sv. Thus all four sections give estimates of
128 ARC transport in the range 44 – 51 Sv across 40-50°E.

129 The cruise 164 and 213 *Discovery* sections allow us to scale up the 1-1500 m *Nansen*
130 transports to full depth transports because all CTDs were full depth. The full depth ARC
131 transports for cruises 164 and 213 were respectively 84.2 Sv (Read and Pollard, 1993)
132 and 71.3 Sv (Pollard and Read, 2001) and the ratios of 1500 m transport to full depth
133 transport are 0.57 and 0.62, average 0.6. Scaling up by 1.67, the *Nansen* estimates of full
134 depth transport are 73.0 Sv at 45°E and 84.7 Sv at 50°E, in close agreement with the
135 previous measurements (71.3 Sv at 42 – 43°E and 84.2 Sv at 41 – 42°E). In summary, we
136 have 4 estimates of full depth ARC transport: 84, 71, 73 and 85 Sv at 41, 42, 45 and 50°E
137 respectively, which closely match two published estimates of the Agulhas Current
138 transport, 73 Sv (Beal and Bryden, 1999) and 85 Sv (Toole and Warren, 1993). Bryden *et al.*
139 (2005), by creating a time series of Agulhas Current transport from moorings that also
140 resolve the Agulhas Undercurrent (Beal and Bryden, 1999), have revised these estimates
141 downwards to 70 ± 21 Sv.

142 We conclude that the data sets discussed here suggest that the Agulhas Current then ARC
143 transport continues unreduced as far as 50°E. Thus significant leakage from the ARC
144 back into the Southwest Indian Ocean subtropical gyre does not begin until east of 50°E.
145 This differs somewhat from previous work (Lutjeharms and Ansorge, 2001). Transferring
146 the northern boundary of the ARC marked on Fig. 3 onto Fig. 2b and extending it along
147 the relevant sea surface height contour (~100 cm, Fig. 2) suggests that northward return
148 flow lies primarily east of Sapmer (say 55°E). There is also some leakage from the
149 cyclonic eddies that regularly break off north from the ARC.

150 For the STF we can do similar calculations. Cruises 164 and 213 yielded STF transports
151 down to 1500 m of 10.5 and 12.5 Sv, 0.53 and 0.89 of the full depth transports 19.8 and
152 14.1 Sv. These compare with 9.6 and 14.5 Sv for the *Nansen* sections. However, the 14.5
153 Sv is rather large, and likely includes a contribution from SAF transport, which cannot be
154 separated. Thus our best estimates of the STF full depth transports remains 14 – 20 Sv
155 from the *Discovery* sections.

156 Our estimate of 9.8 Sv for the SAF transport at 50°E is a minimum, likely enhanced by a
157 contribution from the adjacent STF. At 50°E the SAF is at its northernmost extent at any
158 longitude (Pollard *et al.*, 2007), and there is further transport which has bypassed the
159 meander observed by our short transect and which rejoins further east (Fig. 2b).

3. Closure of the Subtropical Gyre, westward transport

160

161 How the closure of the Subtropical Gyre is achieved is still a subject of active research
 162 (Lutjeharms, 2007). There are three main sources for the Agulhas Current, southward
 163 flow between Mozambique and Madagascar, southwestward flow east of Madagascar and
 164 westward flow between Madagascar and the ARC. Recent research (de Ruijter *et al.*,
 165 2004; de Ruijter *et al.*, 2005) has shown that the first two sources comprise eddies and
 166 dipoles that contribute about 25 Sv (Lutjeharms, 2007; Stramma and Lutjeharms, 1997)
 167 to the Agulhas transport. Examples are apparent in Fig. 2. Arrows on Fig. 2a mark the
 168 paths of a number of eddies that have been tracked from weekly AVISO images for three
 169 months, ending on 18 November 2009, the date of the Fig. 2a image. Focus on the two
 170 anticyclonic eddies just south of Madagascar along 28°S. The eddy at 45°E had formed
 171 and drifted southwestward at 10.7 cm s⁻¹ over three months, then continued
 172 southwestward at 15.2 cm s⁻¹ (Fig. 2b) during the 4-week period between Fig. 2a and Fig.
 173 2b, appearing to form a dipole (de Ruijter *et al.*, 2004) with the cyclonic eddy just west of
 174 it. The eddy at 41°E had drifted westwards at a mean speed of 6.9 cm s⁻¹ over 3 months
 175 (Fig. 2a) and continued west at 12.1 cm s⁻¹ for the next 4 weeks (Fig. 2b) in a dipole with
 176 the cyclonic eddy just north of it. This dipole pair appears to merge with the Agulhas a
 177 week or two after Fig. 2b. The southwestward tracking eddy, on the other hand, appears
 178 to slow down and weaken over the weeks after Fig. 2b, but then drifts west to lose its
 179 momentum to the Agulhas.

180 The third Agulhas source, westward flow between Madagascar and the ARC, is the least
 181 studied and the largest, estimated to be 35-40 Sv down to 1000 m (Lutjeharms, 2007). A
 182 movie of the weekly AVISO images from 2009 up to March 2010 (from which Fig. 2 is
 183 drawn), shows clear westward propagation of eddies (see Fig. 2 for examples), which can
 184 also be seen in Hovmöller diagrams (Boebel *et al.*, 2003; Quartly *et al.*, 2006; Schouten *et al.*,
 185 2002) extracted from the AVISO images (**Fig. 4**). It is now well established that the
 186 westward propagating features are eddies rather than Rossby waves (Chelton *et al.*,
 187 2011), and we shall show that their propagation speeds are in any case larger than can be
 188 attributed to Rossby waves (Killworth *et al.*, 1997). At latitudes 27-33°S westward
 189 propagation is apparent at all longitudes. At 35°S and 37°S the westward propagation
 190 stalls west of about 35°E, countered by the influence of the Agulhas and ARC.

191 The longitude v. time slope of over 60 features has been measured (**Table 2**) to examine
 192 their westward speeds and whether there are variations with time, latitude or longitude.
 193 Splitting the features into two time periods, the first and second halves of the 15 months
 194 plotted in Fig. 4, showed no significant temporal differences, so both time periods have
 195 been merged in Table 2. Westward propagation speeds are similar at all latitudes except
 196 27°S (Table 2), where they are significantly larger. At 27°S, eddies heading west after
 197 rounding the southern tip of Madagascar (as discussed above) lead to larger westward
 198 propagation speeds (12.5 cm s⁻¹) than further south (7.1 cm s⁻¹). Table 2 also shows
 199 significantly larger propagation speeds west of 45°E than east of 45°E at all latitudes.
 200 This divergence is consistent with input of water from the north, from east of
 201 Madagascar, enhancing westward flow.

202 To estimate the strength of inflow from the east, excluding any northern influence, we
 203 therefore restrict ourselves to features south of 27°S and east of 45°E. Table 2 shows
 204 consistent feature propagation of 4.1 ± 0.9 cm s⁻¹ over 40 observations, the standard

205 deviation of the mean being only 0.1 cm s^{-1} . It is interesting to note that, if we integrate
206 the westward speed of 4.1 cm s^{-1} down to 1000m (Lutjeharms, 2007) south from
207 Madagascar to 37°S , the transport would sum to 50 Sv, exceeding Lutjeharm's estimate
208 of 35-40 Sv. Thus the mean westward flow is indeed sufficient to close the transport
209 budget of the Agulhas Current.

210 Between 37°S and 40°S the westward drift interacts with the intense, eastward flowing
211 ARC. The large meanders of the ARC (Boebel *et al.*, 2003) spawn cyclonic eddies to the
212 north of the ARC which propagate west along 37.5°S at an average speed of 5.4 cm s^{-1}
213 (Boebel *et al.*, 2003) until reabsorbed into the next meander trough to the west. Boebel *et al.*
214 found that such eddies were shed nearly exclusively in austral fall (March-May), but
215 the dashed lines around Melville on Fig. 2a show the path of such an eddy which was
216 spawned in early July 2009 and reabsorbed about 6 months later. Another cyclonic eddy
217 southeast of Sapmer can be seen moving west and being reabsorbed in Fig. 2b.

218 In summary, we have shown that eastward transport by the ARC can account for all the
219 transport of the Agulhas Current of 70 Sv (Bryden *et al.*, 2005) as far east as 50°E . East
220 of 50°E , transport begins to peel off to the north to close the gyre circulation. These
221 results update and modify previous conclusions (Lutjeharms and Ansorge, 2001). At all
222 latitudes between the ARC and the southern tip of Madagascar, there is evidence for
223 westward drift of eddies at an estimated speed of 4.1 cm s^{-1} , which suggests a westward
224 transport of as much as 50 Sv, which is sufficient to account for the Agulhas Current
225 transport when added to southward flow of 25 Sv east and west of Madagascar (de Ruijter
226 *et al.*, 2005) and is more than Lutjeharms' estimate of 35-40 Sv of westward flow
227 (Lutjeharms, 2007).

228 4. Circulation near seamounts

229 We end with an overview of how the mean circulation and mesoscale eddies affect the
230 physical structure at each seamount, using both AVISO and *in situ* data. The circulation at
231 each seamount is determined more by its proximity to an eddy than by the weak mean
232 flow, and eddies and their propagation can be determined from Fig. 2. Features in weekly
233 AVISO sea surface height data from July to December 2009 are described. Longer term
234 information on ARC influence at each seamount has been obtained by processing the
235 weekly AVISO images for three years, from 7 January 2009 up to 7 December 2011. For
236 each image, the sea surface height and derived east and north surface velocities have been
237 extracted, at grid points close to each seamount, from the mapped, updated product,
238 yielding 153 week time series at each seamount. The statistics of these time series (**Table**
239 **3**) give an indication of how often each seamount is affected by the ARC. For *in situ* data,
240 we have derived mean profiles at each seamount (**Fig. 5**) by averaging the 24-hour yoyo
241 CTDs at each site.

242 Coral was the only seamount of the survey that was situated south of the ARC and STF
243 but north of the SAF, in the Subantarctic Zone (Pollard *et al.*, 2002) with correspondingly
244 low temperatures and salinities, high oxygens and densities. Between 50 and 100 m
245 stratification was controlled by salinity, with a marked halocline at mean depths between
246 70 and 100 m, and a fresh surface layer. From July 2009 up to the cruise occupation in
247 early December Coral was always in or on the southern side of the STF. Thus eastward
248 circulation of about $10\text{-}20 \text{ cm s}^{-1}$ prevailed. Over three years, the mean surface speed at

249 Coral was 21 cm s^{-1} but reached a maximum of 83 cm s^{-1} proving ARC influence. Speeds
250 over 40 cm s^{-1} occurred about 10% of the time, when anticyclonic meanders of the ARC
251 penetrated south.

252 In July 2009, Melville was located on the northern edge of ARC, at the northern tip of a
253 developing meander that broke off as a cyclonic eddy in August. The eddy (whose path is
254 shown dashed on Fig. 2a) moved a small distance north then west (Fig. 2a) such that
255 Melville lay on its western then southern then eastern edge. By November, the meander
256 that spawned the eddy had moved east until it was south of MoW (Fig. 2). In early
257 January 2010 the eddy remerged with the next westward meander of the ARC to the one
258 which spawned it (Boebel *et al.*, 2003). When the site was occupied in December,
259 altimeter derived velocities were approximately 20 cm s^{-1} to the southwest (Fig. 2b).
260 Melville is the closest seamount to the core of the ARC, so shows the highest mean (34
261 cm s^{-1}) and maximum (94 cm s^{-1}) speeds and variability over three years (Table 3).
262 Speeds were greater than 40 cm s^{-1} over 30% of the time.

263 MoW most often lies on the northern flank of the ARC, and did so for several months
264 after mid-December 2009 (Fig. 2b). In October and November 2009, however, MoW lay
265 near the edge of an anticyclonic eddy that formed in August between two northward
266 meanders of the ARC, then moved slowly to the northwest from October. During the
267 survey, MoW lay on the south side of the elongated centre of the eddy (Fig. 2b), in
268 southeast to east currents of up to 30 cm s^{-1} . MoW lies about as far north of the core of
269 the ARC as Coral lies south, so shows similar statistics (Table 3), being affected by
270 northward penetrating cyclonic meanders of the ARC, which resulted in speeds of 40 cm
271 s^{-1} being exceeded 16% of the time.

272 The anticyclonic eddy which influenced MoW in late 2009 also affected Sapmer (on its
273 northwest flank) from early September 2009, being centred on Sapmer in mid-November
274 (Fig. 2a), and continued to affect Sapmer, on its southeast flank, until late January 2010.
275 Thus, when Sapmer was occupied on 22 - 24 November (Table 1), the presence of the
276 eddy resulted in remarkably weak stratification (Fig. 5c) down to over 400 m (i.e. below
277 the crest of the seamount). Note the relatively high oxygens down to 400 m at Sapmer,
278 hinting at deep mixing from the surface. The sea surface height at Sapmer during the
279 cruise (nearly 130 cm, Fig. 2b) was the highest over three years, showing that the eddy
280 was the strongest, but there were six sea surface height maxima in that period, of which
281 two reached 120 cm, so that mesoscale eddies regularly affect that site. However, Sapmer
282 is too far north to be directly influenced by the ARC, with surface current speeds always
283 less than 40 cm s^{-1} .

284 Atlantis and Walter seamounts are both several degrees north of the other seamounts,
285 hence have greater near-surface stratification (Fig. 5c). Atlantis sees a slow westward
286 drift of weak, mostly cyclonic eddies. During the cruise, a weak anticyclone to the
287 southeast of Atlantis gave rise to small ($<20 \text{ cm s}^{-1}$) currents at the surface in a west to
288 southwesterly direction. Walter, on the other hand, was situated just to the southeast of
289 the track of rapidly translating eddies from east of Madagascar. One of these anticyclonic
290 eddies of light, tropical water lay to the north and a second, slow-moving cyclonic eddy
291 of denser, subtropical water had moved to the south of Walter by the time it was surveyed
292 (Fig. 2b). Hence flow past the seamount was to the east averaging 20 cm s^{-1} . Over three
293 years, Walter shows slightly higher current statistics than Atlantis, because it is regularly

294 affected by the eddies propagating south from East of Madagascar. Oxygens are
295 particularly low at Walter as a result of the southward flow of low-oxygen water.

296 Comparing properties at the six seamounts (Fig. 5), all but Coral have near-identical
297 water masses in the thermocline (Fig. 5f), but isopycnals in the thermocline (say 26.4 kg m^{-3} ,
298 Fig. 5c) are shallowest at Coral and Atlantis, the southern and northeast corners of
299 the survey respectively. This reflects the strong eastward flow of the ARC north of Coral,
300 but more interestingly, confirms the westward drift between Atlantis and the seamounts
301 near the ARC. Oxygen values (Fig. 5d) at all but two seamounts increase towards the
302 surface, indicating that the spring bloom and summer stratification have not taken hold.
303 At Atlantis and Walter the decrease in oxygen above 50 m matches the strong near-
304 surface stratification (Fig. 5c). Fluorescence at all seamounts, although uncalibrated, was
305 very low, but in all cases there was a subsurface peak, close to 100 m deep at Atlantis and
306 Walter, shallower at all other seamounts.

307

5. Conclusions

308 We have shown that the Agulhas Current transport can all be accounted for in the
309 Agulhas Return Current, flowing eastwards to 50°E , with large meanders, between 37°S
310 and 41°S . This transport, $71 - 85 \text{ Sv}$, results in surface currents up to about 100 cm s^{-1}
311 within the core of the ARC. The subtropical front carries a further $14 - 20 \text{ Sv}$. Three of
312 the six seamounts surveyed, Coral, Melville and MoW, are strongly influenced by the
313 ARC, experiencing surface currents of over 40 cm s^{-1} during 10%, 30% and 16% of a
314 three year period, respectively. These currents occur either when the seamount is in the
315 core of the ARC or in mesoscale eddies that regularly spin off the ARC.

316 North of the ARC a large number of mesoscale eddies are observed, in general
317 propagating westwards at mean speeds of $4.1 \pm 0.9 \text{ cm s}^{-1}$. From this westward drift, a
318 westward transport of up to 50 Sv has been estimated, which, together with 25 Sv of
319 southward transport east and west of Madagascar (Lutjeharms, 2007), accounts for the 70
320 $\pm 21 \text{ Sv}$ Agulhas transport (Beal and Bryden, 1999). All the seamounts surveyed are
321 influenced by eddies on occasion, resulting in mean currents past a seamount of up to 30
322 $- 50 \text{ cm s}^{-1}$.

323 Stratification in the upper 400 m varied considerably between the six seamounts. It was
324 largest at Walter and Atlantis, the northernmost sites, and weakest at Sapmer, because
325 Sapmer was in the centre of a deep-extending anticyclonic eddy when it was surveyed.

326

Acknowledgements

327 The authors would like to thank the officers, crew and scientists of the RV Dr Fridtjof
328 Nansen cruise 2009 410 without whose help these data would not have been collected.
329 This work was supported by the NERC large scale observing programme.

330

Tables

331

Table 1 – Seamounts surveyed

Seamount	Atlantis	Sapmer	Middle of What	Coral	Melville	W of Walters Shoal
Latitude °S	32.6-32.9	36.7-37.0	37.8-38.1	41.3-41.6	38.3-38.6	31.5-31.8
Longitude °E	57.1-57.5	51.9-52.3	50.2-50.6	42.7-43.1	46.5-46.9	42.65-43.05
Minimum depth depth of CTD yoyo	750 m (70m min)	350 m	1100m	200 m	100 m	1250 m
dates occupied	17-19Nov	22-24Nov	25-27Nov	2-4Dec	7-10Dec	12-13Dec
jdays occupied	321-323	326-328	329-331	336-338	341-344	346-347

332

333

334

335

Table 2 – Westward speeds of eddy propagation

Latitude °S	Features west of 45°E			Features east of 45°E		
	Mean cm/s	Standard deviation	Number in sample	Mean cm/s	Standard deviation	Number in sample
27	12.5	0.8	2	7.3	1.7	4
29	7.8	1.2	5	4.2	1.3	7
31	8.4	1.5	6	4.2	1.1	6
33	7.1	0.4	3	4.3	0.6	8
35	5.7	1.7	5	4.3	0.8	10
37	5.5	0.6	2	3.7	0.7	9
29-37	7.1	1.7	21	4.1	0.9	40

336

337

Table 3 – Statistics of surface speeds (cm s⁻¹) near each seamount

seamount	Mean speed	Standard deviation	Maximum speed
Atlantis	12	6	27
Sapmer	15	9	39
MoW	23	17	85
Coral	21	15	83
Melville	34	22	93
Walter	18	9	50

338

339

340

Figures

- 341 Fig. 1 The positions of the six seamounts surveyed during the Nansen cruise are shown
342 relative to the bathymetry of the Southwest Indian Ocean and a streamline of the
343 Agulhas Return Current (dashed, see Fig. 2). Five of the seamounts – Atlantis,
344 Sapmer, Middle of What (MoW), Melville and Coral lay along the SouthWest
345 Indian Ridge (SWIR) and Walter was on the west side of the Madagascar Ridge.
346 Sapmer, MoW, Melville and Coral all lay close to the path of the Agulhas Return
347 Current.
- 348 Fig. 2 AVISO sea surface height (SSH) maps are shown for (a) 18 Nov (b) 16 Dec 2009,
349 four weeks apart and close to the start (17 Nov, Atlantis) and end (13 Dec, Walter)
350 of the survey. Arrows show the paths of eddies tracked with weekly SSH maps.
351 Numbers are speeds in cm/sec. In (a), arrows show distance travelled in 91 days (3
352 months) from 19 Aug to 18 Nov. In (b), arrows show the distance travelled by the
353 same features in the 4-week period from 18 Nov to 16 Dec. Dashed lines in (a)
354 show path of cyclonic eddy that broke off ARC from when it was spawned around
355 8 July to when it coalesced back onto another meander around 20 Jan 2010 after
356 6 months. Crosses mark CTD and seamount positions. Agulhas Return Current
357 (ARC), SubTropical Front (STF) and SubAntarctic Front (SAF) are marked.
- 358 Fig. 3 Heavy dashes mark the boundaries of the Agulhas Return Current (ARC),
359 Subtropical Front (STF) and SubAntarctic Front (SAF) as determined from
360 salinity, temperature and depth range criteria (Belkin and Gordon, 1996) along the
361 two closely spaced CTD sections. Between the sections, the dashed lines are
362 superimposed on sea surface height streamlines from satellite altimetry closest in
363 time to our occupation of the sections (Fig. 2b). Eastward transport (S_v) is
364 annotated for each station pair and summed for each front.
- 365 Fig. 4 Hovmöller plots of AVISO sea surface height against longitude and time show
366 westward propagation of features at all latitudes between Madagascar and the
367 ARC. Westward propagation ceases only close to the Agulhas and in the vicinity
368 of the Agulhas retroflexion.
- 369 Fig. 5 Profiles of (a) potential temperature, (b) salinity, (c) density, (d) oxygen, (e)
370 fluorescence against depth and (f) potential temperature against salinity at each
371 seamount, averaged over 24 hours. Averages of properties including depth were
372 calculated on density surfaces then plotted against the averaged depth, in order to
373 avoid smoothing of features which can result from normal depth averaging. The
374 most pronounced differences were at Coral (blue) where the depth averaged
375 profiles are shown dashed for comparison. Depth averaging is more reliable near
376 the surface and bottom of each profiles. Oxygen and fluorescence are not
377 absolutely calibrated, for lack of calibration data, but depth dependent features are
378 of interest. Subtropical Surface Water (STSW) and Subantarctic Surface Water
379 (SASW) are marked on (f).

380

References

- 381 Beal, L.M., Bryden, H.L., 1999. The velocity and vorticity structure of the Agulhas
382 Current at 32°S. *Journal of Geophysical Research* 104 (C3), 5151-5176.
- 383 Belkin, I.M., Gordon, A.L., 1996. Southern Ocean fronts from the Greenwich Meridian to
384 Tasmania. *Journal of Geophysical Research* 101 (C2), 3675-3696.
- 385 Boebel, O., Rossby, T., Lutjeharms, J., Zenk, W., Barron, C., 2003. Path and variability
386 of the Agulhas Return Current. *Deep Sea Research Part II: Topical Studies in*
387 *Oceanography* 50 (1), 35-56.
- 388 Bryden, H.L., Beal, L.M., Duncan, L.M., 2005. Structure and transport of the Agulhas
389 Current and its temporal variability. *Journal of Oceanography* 61 (3), 479-492.
- 390 Chelton, D.B., Schlax, M.G., Samelson, R.M., 2011. Global observations of nonlinear
391 mesoscale eddies. *Progress in Oceanography* 91 (2), 167-216.
- 392 de Ruijter, W.P.M., Aken, H.M.v., Beier, E.J., Lutjeharms, J.R.E., Matano, R.P.,
393 Schouten, M.W., 2004. Eddies and dipoles around South Madagascar: formation,
394 pathways and large-scale impact. *Deep Sea Research Part I: Oceanographic*
395 *Research Papers* 51 (3), 383-400.
- 396 de Ruijter, W.P.M., Ridderinkhof, H., Schouten, M.W., 2005. Variability of the
397 southwest Indian Ocean. *Philosophical Transactions of the Royal Society A:*
398 *Mathematical, Physical and Engineering Sciences* 363 (1826), 63-76.
- 399 Killworth, P.D., Chelton, D.B., de Szoeke, R.A., 1997. The Speed of Observed and
400 Theoretical Long Extratropical Planetary Waves. *Journal of Physical*
401 *Oceanography* 27 (9), 1946-1966.
- 402 Lutjeharms, J.R.E., 2006. *The Agulhas Current*. Springer, Berlin.
- 403 Lutjeharms, J.R.E., 2007. Three decades of research on the greater Agulhas Current.
404 *Ocean Science* 3, 129-147.
- 405 Lutjeharms, J.R.E., Ansorge, I.J., 2001. The Agulhas Return Current. *Journal of Marine*
406 *Systems* 30 (1-2), 115-138.
- 407 Pollard, R.T., Lucas, M.I., Read, J.F., 2002. Physical controls on biogeochemical
408 zonation in the Southern Ocean. *Deep-Sea Research II* 49 (16), 3289-3305.
- 409 Pollard, R.T., Read, J.F., 2001. Circulation pathways and transports of the Southern
410 Ocean in the vicinity of the Southwest Indian Ridge. *Journal of Geophysical*
411 *Research* 106 (C2), 2881-2898.
- 412 Pollard, R.T., Venables, H.J., Read, J.F., Allen, J.T., 2007. Large scale circulation around
413 the Crozet Plateau controls an annual phytoplankton bloom in the Crozet Basin.
414 *Deep-Sea Research II* 54 (18-20), 1915-1929,
415 doi:1910.1016/j.dsr1912.2007.1906.1012.
- 416 Quartly, G.D., Buck, J.J.H., Srokosz, M.A., Coward, A.C., 2006. Eddies around
417 Madagascar -- The retroflexion re-considered. *Journal of Marine Systems* 63 (3-
418 4), 115-129.

- 419 Read, J.F., Lucas, M.I., Holley, S.E., Pollard, R.T., 2000. Phytoplankton, nutrients and
420 hydrography in the frontal zone between the Southwest Indian subtropical gyre
421 and the Southern Ocean. *Deep-Sea Research I* 47 (12), 2341-2367.
- 422 Read, J.F., Pollard, R.T., 1993. Structure and transport of the Antarctic Circumpolar
423 Current and Agulhas Return Current at 40°E. *Journal of Geophysical Research* 98
424 (C7), 12281-12295.
- 425 Schouten, M.W., de Ruijter, W.P.M., van Leeuwen, P.J., 2002. Upstream control of
426 Agulhas Ring shedding. *Journal of Geophysical Research* 107 (C8), 3109.
- 427 Stramma, L., Lutjeharms, J.R.E., 1997. The flow field of the subtropical gyre of the South
428 Indian Ocean. *Journal of Geophysical Research* 102 (C3), 5513-5530.
- 429 Toole, J.M., Warren, B.A., 1993. A hydrographic section across the subtropical South
430 Indian Ocean. *Deep-Sea Research* 40 (10), 1973-2019.
- 431
- 432

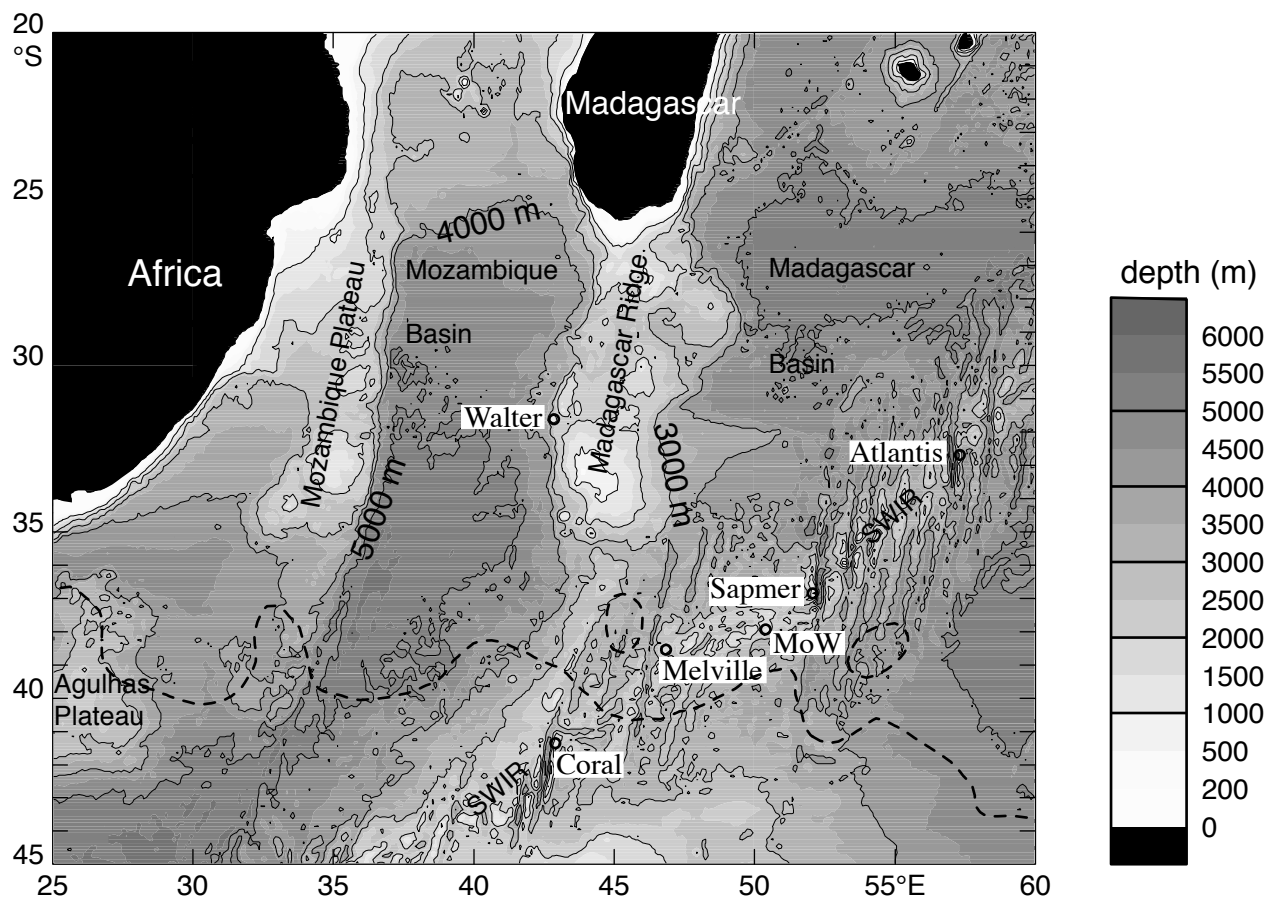


Fig. 1 The positions of the six seamounts surveyed during the Nansen cruise are shown relative to the bathymetry of the Southwest Indian Ocean and a streamline of the Agulhas Return Current (dashed, see Fig. 2). Five of the seamounts – Atlantis, Sapmer, Middle of What (MoW), Melville and Coral lay along the SouthWest Indian Ridge (SWIR) and Walter was on the west side of the Madagascar Ridge. Sapmer, MoW, Melville and Coral all lay close to the path of the Agulhas Return Current.

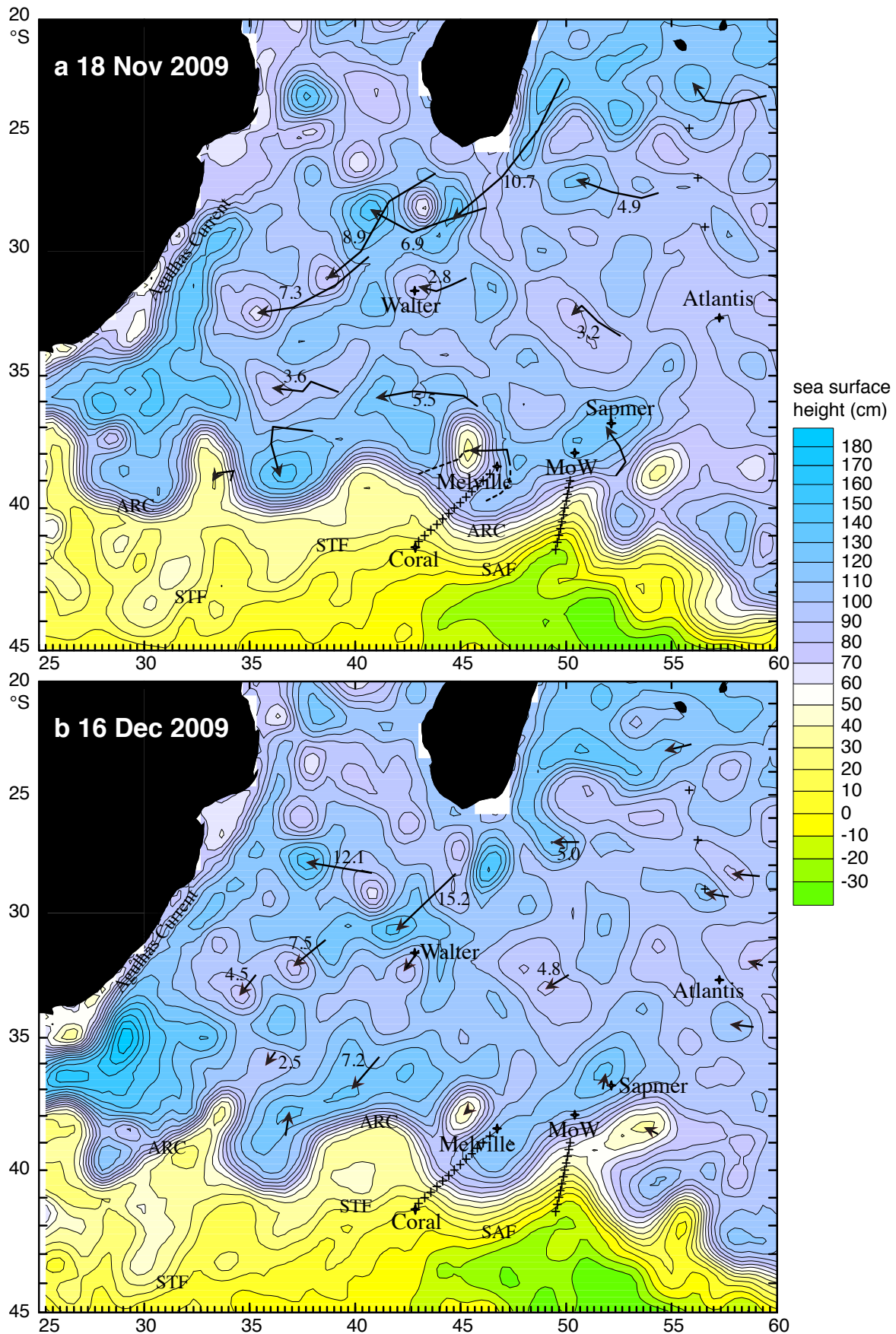


Fig. 2 AVISO sea surface height (SSH) maps are shown for (a) 18 Nov (b) 16 Dec 2009, four weeks apart and close to the start (17 Nov, Atlantis) and end (13 Dec, Walter Shoals) of the survey. Arrows show the paths of eddies tracked with weekly SSH maps. Numbers are speeds in cm/sec. In (a), arrows show distance travelled in 91 days (3 months) from 19 Aug to 18 Nov. In (b), arrows show the distance travelled by the same features in the 4-week period from 18 Nov to 16 Dec. Dashed lines in (a) show path of cyclonic eddy that broke off ARC from when it was spawned around 8 July to when it coalesced back onto another meander around 20 Jan 2010 after 6 months. Crosses mark CTD and seamount positions. Agulhas Return Current (ARC), SubTropical Front (STF) and SubAntarctic Front (SAF) are marked.

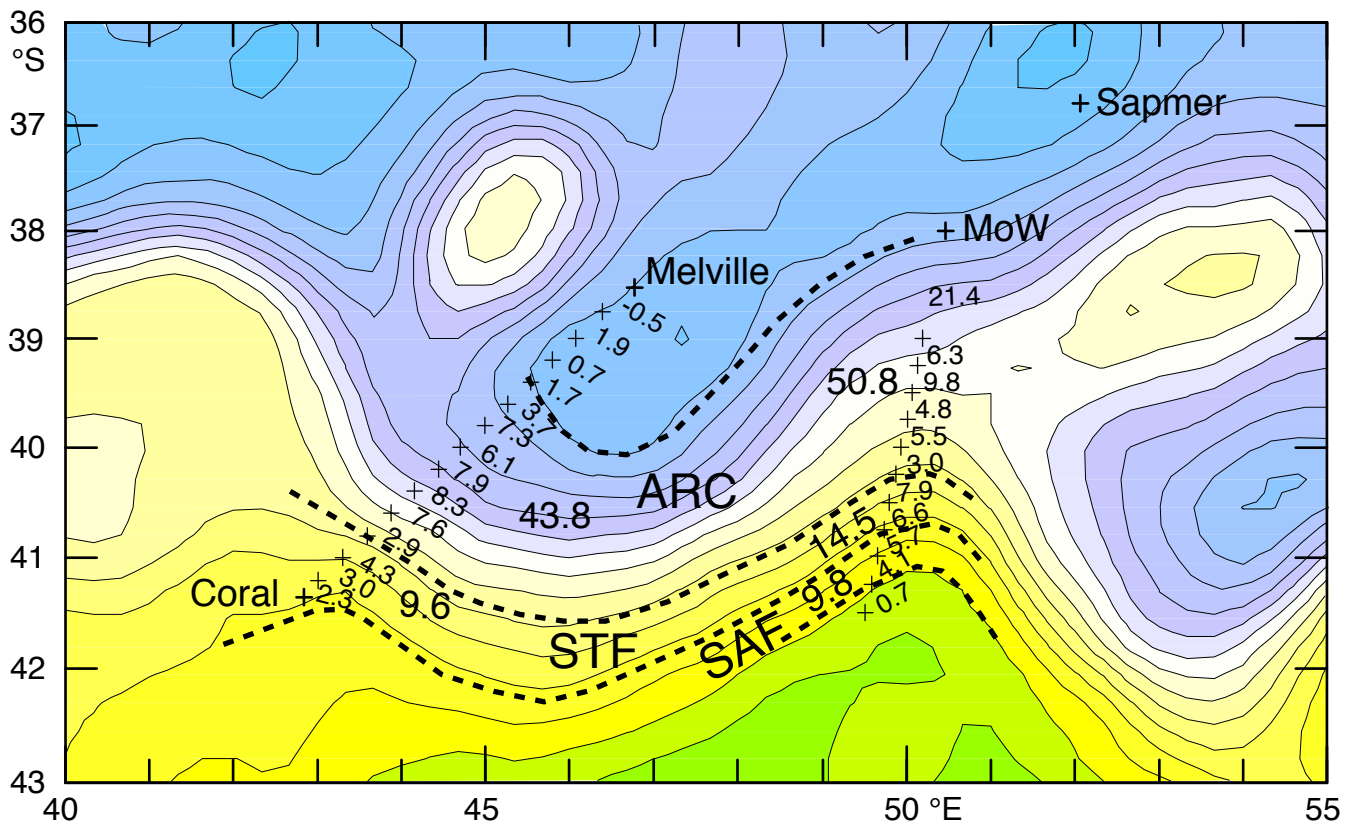


Fig. 3 Heavy dashes mark the boundaries of the Agulhas Return Current (ARC), Subtropical Front (STF) and SubAntarctic Front (SAF) as determined from salinity, temperature and depth range criteria (Belkin and Gordon, 1996) along the two closely spaced CTD sections. Between the sections, the dashed lines are superimposed on sea surface height streamlines from satellite altimetry closest in time to our occupation of the sections (Fig. 2b). Eastward transport (S_v) is annotated for each station pair and summed for each front.

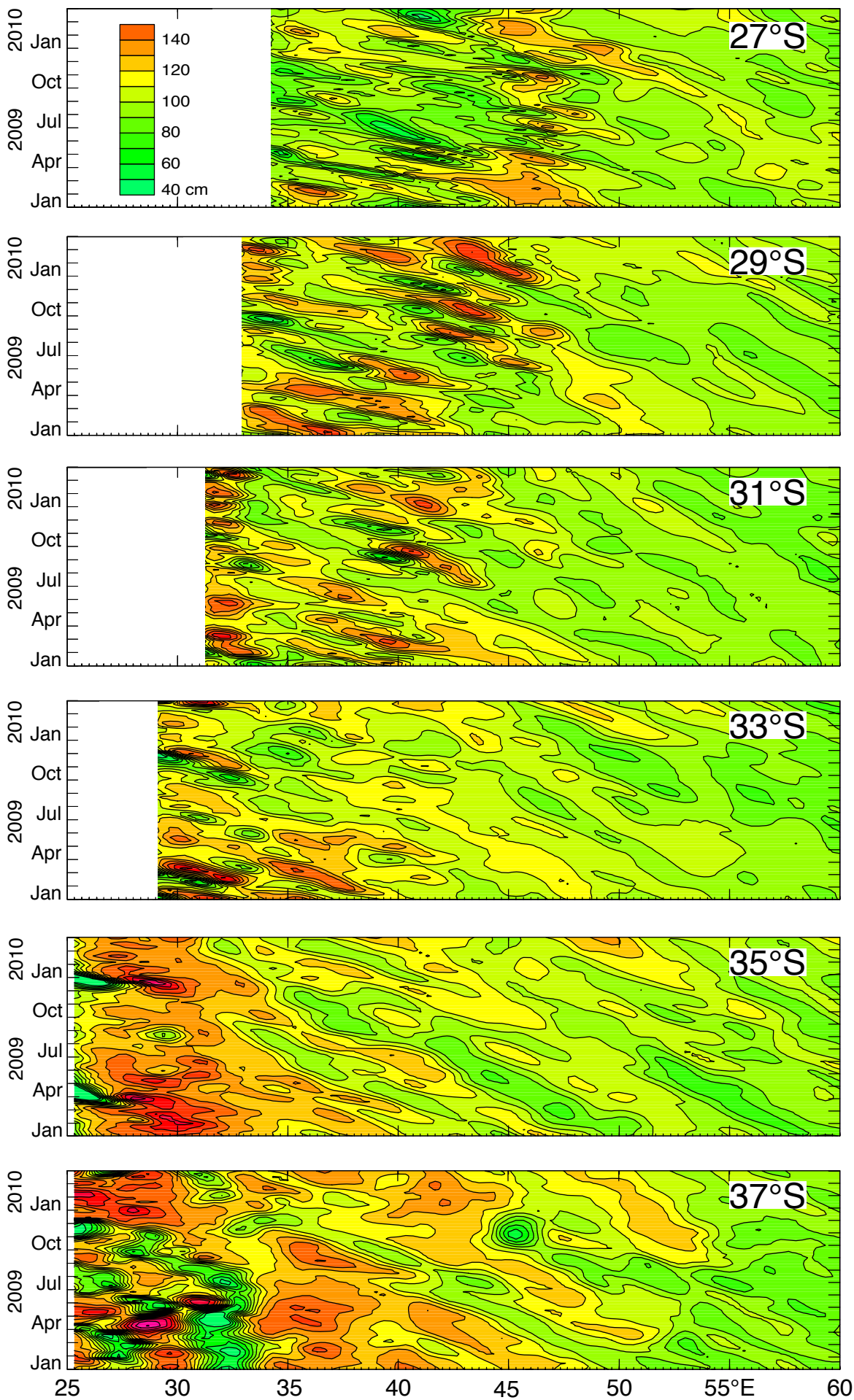


Fig. 4 Hovmöller plots of AVISO sea surface height against longitude and time show westward propagation of features at all latitudes between Madagascar and the ARC. Westward propagation ceases only close to the Agulhas and in the vicinity of the Agulhas retroflection.

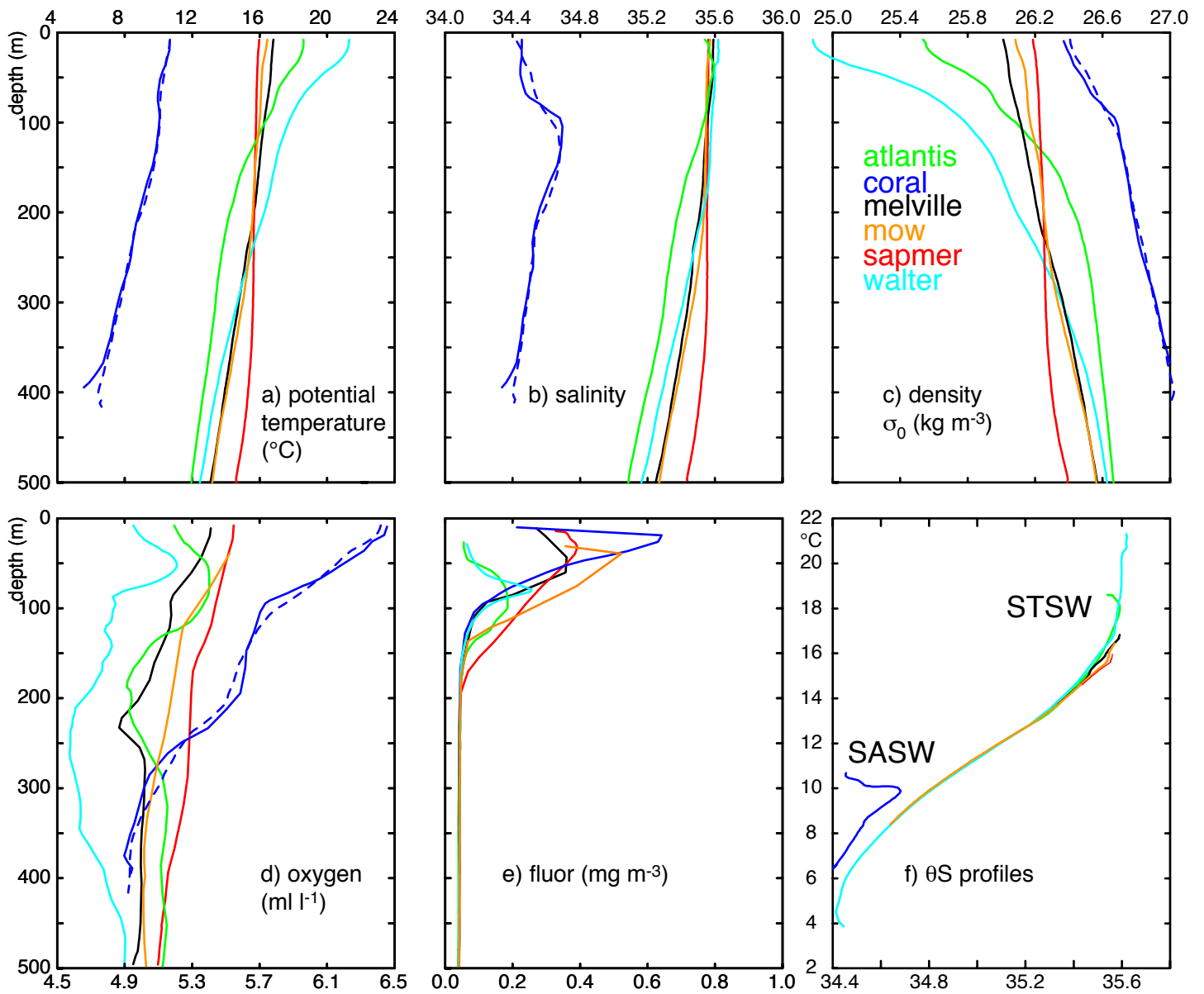


Fig. 5 Profiles of (a) potential temperature, (b) salinity, (c) density, (d) oxygen, (e) fluorescence against depth and (f) potential temperature against salinity at each seamount, averaged over 24 hours. Averages of properties including depth were calculated on density surfaces then plotted against the averaged depth, in order to avoid smoothing of features which can result from normal depth averaging. The most pronounced differences were at Coral (blue) where the depth averaged profiles are shown dashed for comparison. Depth averaging is more reliable near the surface and bottom of each profiles. Oxygen and fluorescence are not absolutely calibrated, for lack of calibration data, but depth dependent features are of interest. Subtropical Surface Water (STSW) and Subantarctic Surface Water (SASW) are marked on (f).